Citation: Cell Death and Disease (2012) 3, e445; doi:10.1038/cddis.2012.182

www.nature.com/cddis

Functional cooperativity by direct interaction between PAK4 and MMP-2 in the regulation of anoikis resistance, migration and invasion in glioma

D Kesanakurti[1], C Chetty[1], D Rajasekhar Maddirela[1], M Gujrati[2] and JS Rao*[,1,3]

Gliomas display anoikis resistance, enhanced invasion in to the adjacent brain parenchyma and eventually recur despite using the standard therapies. Our studies on increased anoikis sensitization in matrix metalloproteinase-2 (MMP-2)-knockdown 4910 and 5310 human glioma xenograft cells were interestingly correlated with p21-activated kinase 4 (PAK4) inhibition, prompting us to further investigate the role of PAK4 in glioma. Here, we report the PAK4 upregulation in positive correlation with increasing glioma pathological grades. The siRNA-mediated PAK4 knockdown elevated anoikis, and inhibited invasion and migration by downregulating MMP-2, $\alpha v\beta 3$-integrin and phospho-epidermal growth factor receptor (phospho-EGFR). The cDNA-PCR arrays revealed a transcriptional suppression of essential proteins involved in cell proliferation and adhesion in PAK4-knockdown cells. Most importantly, glutathione S-transferase pull-down assays demonstrated the MMP-2 as a new PAK4-interacting protein which binds to PAK4 kinase domain. Individual EGFR/ErbB2 inhibitor and $\alpha v\beta 3$ antibody treatments in PAK4si-treated cells indicated the regulation of $\alpha v\beta 3$/EGFR survival signaling by PAK4. Overexpression of PAK4 significantly reversed the MMP2si-induced cell death in both cell lines. Codepletion of PAK4 and MMP-2 resulted in robust anoikis-mediated cell death, and severely inhibited invasive and migratory properties in these cells. PAK4si inhibited *in vivo* tumor growth in nude mice by inhibiting MMP-2, $\beta 3$-integrin and phospho-EGFR levels in tumors. Our findings indicate a physical association between PAK4 and MMP-2, and suggest the future therapeutic potential of PAK4/MMP-2 dual targeting in glioma treatment.
Cell Death and Disease (2012) **3,** e445; doi:10.1038/cddis.2012.182; published online 20 December 2012
Subject Category: Cancer

Glioblastoma multiforme (GBM) is the most malignant human intracerebral neoplasms, which display robust proliferation, resistance to detachment-induced cell death, diffused invasion into the adjacent brain parenchyma and result in escape of tumor cells to the standard polychemo and radiotherapies after surgical resection.[1,2] Metastasis is a multiphase process including the dissociation of cancer cells from the site of origin, travel through circulatory and lymphatic systems, dissemination and proliferation in distant target organs.[3] As a result of loss of integrin-mediated extracellular matrix (ECM) contact or inappropriate cell-to-cell interactions, cells undergo anoikis, a form of detachment-induced apoptosis which has an important role in normal physiological and developmental processes in organisms. However, acquiring anoikis resistance is a hallmark of malignantly transformed cancer cells to survive in an anchorage-independent manner.[4,5] Integrins are transmembrane receptors, which comprise 18 α- and 8 β-subunits that combine to form at least 24 heterodimers. GBM malignancy is in part attributed to aberrant integrin expression.[6] Integrins are critical mediators of cell–ECM interactions that transduce extracellular signals into the intracellular network through integrin-mediated signaling molecules, including epidermal growth factor receptor (EGFR), focal adhesion kinase (FAK) and phosphatidylinositol 3-kinase (PI3K).[5,7]

The role of matrix metalloproteases (MMPs) is significant in the degradation of ECM, thereby facilitating tumor cell invasion.[1] Matrix metalloproteinase-2 (MMP-2) is a 72 kDa, Zn^{+2}-dependent secreted or membrane-bound endopeptidase with potential multiple roles in cell proliferation, migration, invasion and angiogenesis.[8] Our preliminary studies on enhanced anoikis in MMP-2-knockdown human glioma xenograft cells were surprisingly correlated with the significant inhibition in p21-activated kinase 4 (PAK4) levels. PAKs constitute a family of downstream effectors of small Rho GTPases Rac1 and Cdc42, which has diverse cellular functions by regulating cytoskeletal reorganization, cell survival and angiogenesis.[9,10] PAK4 was initially identified as a Cdc42H effector molecule and suggested to participate in actin cytoskeleton reorganization and filopodia formation.[11–13] Aberrant PAK4 expression was implied to be associated with enhanced tumor progression in ovarian, colon, prostate, gastric, breast cancers, choriocarcinoma and hepatocellular carcinomas.[14,15] However, a possible PAK4 upregulation and

[1]Department of Cancer Biology and Pharmacology, University of Illinois College of Medicine, Peoria, IL, USA; [2]Department of Pathology, University of Illinois College of Medicine, Peoria, IL, USA and [3]Department of Neurosurgery, Department of Pathology, University of Illinois College of Medicine, Peoria, IL, USA
*Corresponding author: JS Rao, Department of Cancer Biology and Pharmacology, University of Illinois College of Medicine, One Illini Drive, Peoria, IL 61605, USA. Tel: +309 671 3445; Fax: +309 671 3442; E-mail: jsrao@uic.edu
Keywords: anoikis; $\alpha v\beta 3$ integrin; EGFR; MMP-2; PAK4; kinase domain
Abbreviations: DAPI, 4′,6-diamidino-2-phenylindole; EGFR, epidermal growth factor receptor; FAK, focal adhesion kinase; PI3K, phosphatidylinositol 3-kinase; MMP-2, matrix metalloproteinase 2; PAK4, p21-activated kinase 4; PI, propidium iodide; CRIB, Cdc42Hs/Rac-interactive binding domain; GID, GEF–H1 interaction domain; IBD, integrin-binding domain
Received 03.7.12; revised 10.10.12; accepted 29.10.12; Edited by A Verkhratsky

oncogenic role in glioma still remains incompletely defined. EGFR signaling has a key role in maintaining GBM hallmark characteristics, including rapid cell proliferation, diffuse invasion and metastases.[16] A possible cross-talk between PAK4 and EGFR was suggested to enhance malignancy in ovarian cancer.[13]

To our knowledge, this is the first comprehensive study demonstrating the PAK4 upregulation in positive correlation with increasing glioma pathological grades. Most importantly, our experiments demonstrated that MMP-2 directly interacts with PAK4 and augments the activation of $\alpha v\beta 3$-mediated EGFR prosurvival signaling. On the other hand, cosuppression of PAK4 and MMP-2 conferred anoikis-mediated cell death in cells and inhibited *in vivo* tumor growth, thereby suggests the therapeutic potential of PAK4/MMP-2 dual targeting in glioma treatment.

Results

MMP-2-knockdown sensitized glioma xenograft cells to anoikis and inhibited invasion and migration. Characteristics of anchorage-independent growth and anoikis resistance in tumor cells are central for augmented tumor malignancy. Specific knockdown studies were performed using MMP2si in cells grown as either adhered monolayers (Adh) or in suspension (Sus). MMP-2-knockdown resulted in ~42.3% death in adhered cells and more sensitized to anoikis-mediated cell death (~62.4%) in suspended cells compared with the corresponding controls (Figure 1a). Cleavage of PARP, caspase-8 and caspase-3 also confirmed the MMP2si-induced anoikis in suspension (Figure 1b). FACS analysis revealed an increased apoptotic cell percentage in the sub/G_1 phase in MMP2si-treated adhered cells (4910, ~29.1%; 5310, ~28.4%). However, MMP-2si significantly elevated the apoptotic cell proportion (4910, ~53.6%; 5310, ~51.1%) in suspension cultures (Figure 1c). We also observed conspicuous changes in cell morphology leading to cell rounding, withdrawal of cellular foci and increased percentage of rounded cells (~62%) after 48 h in MMP2si-treated cells (Figure 1d). Further, MMP-2 knockdown resulted in significant inhibition in cell adhesion on vitronectin (VN; 4910, ~60.3%; 5310, ~60.6%) and fibronectin (FN; 4910, ~53.3%; 5310, ~50.8%) compared with controls (Figure 1e). MMP-2 suppression resulted in ~59.8% loss of invasive potential in both cell lines (Figure 1f). Consistently, wound-healing migration assay confirmed the decreased ability of MMP2si-treated cells to migrate and close the wound compared with controls (Figure 1g). To determine the potential molecular intermediates contributing to MMP2si-induced anoikis and loss of migration, we performed immunoblotting using whole adhered and suspended cell lysates. In adhered MMP2si-treated cells, we observed a substantial phospho-PAK4 and total-PAK4 downregulation accompanied by decreased phospho-EGFR, phospho-c-Src and phospho-FAK levels, which were further drastically decreased in suspended cultures compared with respective controls (Figure 1h). These results suggested the potential MMP-2 role in anchorage-independent growth and escaping anoikis in these cell lines.

PAK4 is overexpressed in glioma. A detailed expression analysis and functional characterization studies of PAK4 in pathological relevance to glioma malignancy are still lacking. The PAK4 mRNA levels were significantly upregulated in SNB19, U251, U87MG, 4910 and 5310 glioma cell lines compared with normal human brain astrocytes, which showed very less or no PAK4 expression (Figure 2a). Both PAK4 and phospho-PAK4 levels were elevated in these cells, whereas brain astrocytes did not show any noticeable expression (Figure 2b). Immunohistochemistry on human GBM tissue microarrays revealed a widespread, elevated PAK4 expression in gliomas. The normal brain (NB) and tumor-adjacent NB (ANB) tissues did not show significant PAK4 expression (Figure 2c). We observed a moderate PAK4 expression in grade-II and a high expression in grade-III and -IV tumors. A positive correlation between PAK4 expression and increasing glioma pathogenesis was observed (Figure 2d). Consistently, studies with grade-II ($n=17$) and grade-IV ($n=15$) patient biopsies also showed significant mRNA upregulation in tumors (Supplementary Figure S1A). Western blotting (WB) indicated moderate and high expression levels of phospho-PAK4 and PAK4 in grade-II and grade-IV tumor biopsies, respectively, whereas NB tissues did not display any significant expression (Supplementary Figure S1B). Immunohistochemical (IHC) analysis also confirmed elevated PAK4 positivity in grade-II and grade-IV tumors (Supplementary Figure S1C). These results strongly imply the potential oncogenic role of PAK4 in glioma initiation and progression.

PAK4 is required for anoikis resistance, cell adhesion, invasion and migration in glioma xenograft cells. To further investigate the possible role of PAK4 in glioma malignancy, we studied the consequences of siRNA-mediated PAK4 downregulation. PAK4si significantly decreased the PAK4 mRNA levels (4910, ~71.3%; 5310, ~70.7%) (Figure 3a). PAK4 (4910, ~68.3%; 5310, ~67.9%) and phospho-PAK4 levels were significantly decreased in PAK4si-treated cells compared with mock or scrambled controls (Figure 3b). In adhered conditions, PAK4-knockdown cells showed decreased cell viability (~42.5%) compared with pSV controls. On the other hand, the basal anoikis levels in suspension-cultured pSV-treated cells (~11%) were dramatically increased, up to 67%, in PAK4-deficient cells (Figure 3c). PAK4.si-treated cells showed significant inhibition in colony-forming ability (4910, ~74.1%; 5310, ~73.5%) in these cells (Supplementary Figures S2A and B). Cell-adhesion assays on VN (4910, ~76%; 5310, ~74%) and FN (4910, ~70.5%; 5310, ~70%) revealed the noticeable PAK4si inhibitory effect on adhesion to ECM (Figure 3d). The prominent morphological changes associated with cell rounding, withdrawal of cellular foci and surface detachment leading to anoikis were observed in PAK4si-treated cells. Although these characteristics were also observed at the end of 24 h, a conspicuous inhibitory effect was evident after 48 h (~68%) of PAK4si treatment (Figure 3e). Consistent with these results, the invasiveness was inhibited (~61%) in PAK4si-treated cells (Figure 3f). Similarly, wound-healing assays revealed inhibited migratory potential and wound closure in PAK4si-treated cells (Figure 3g).

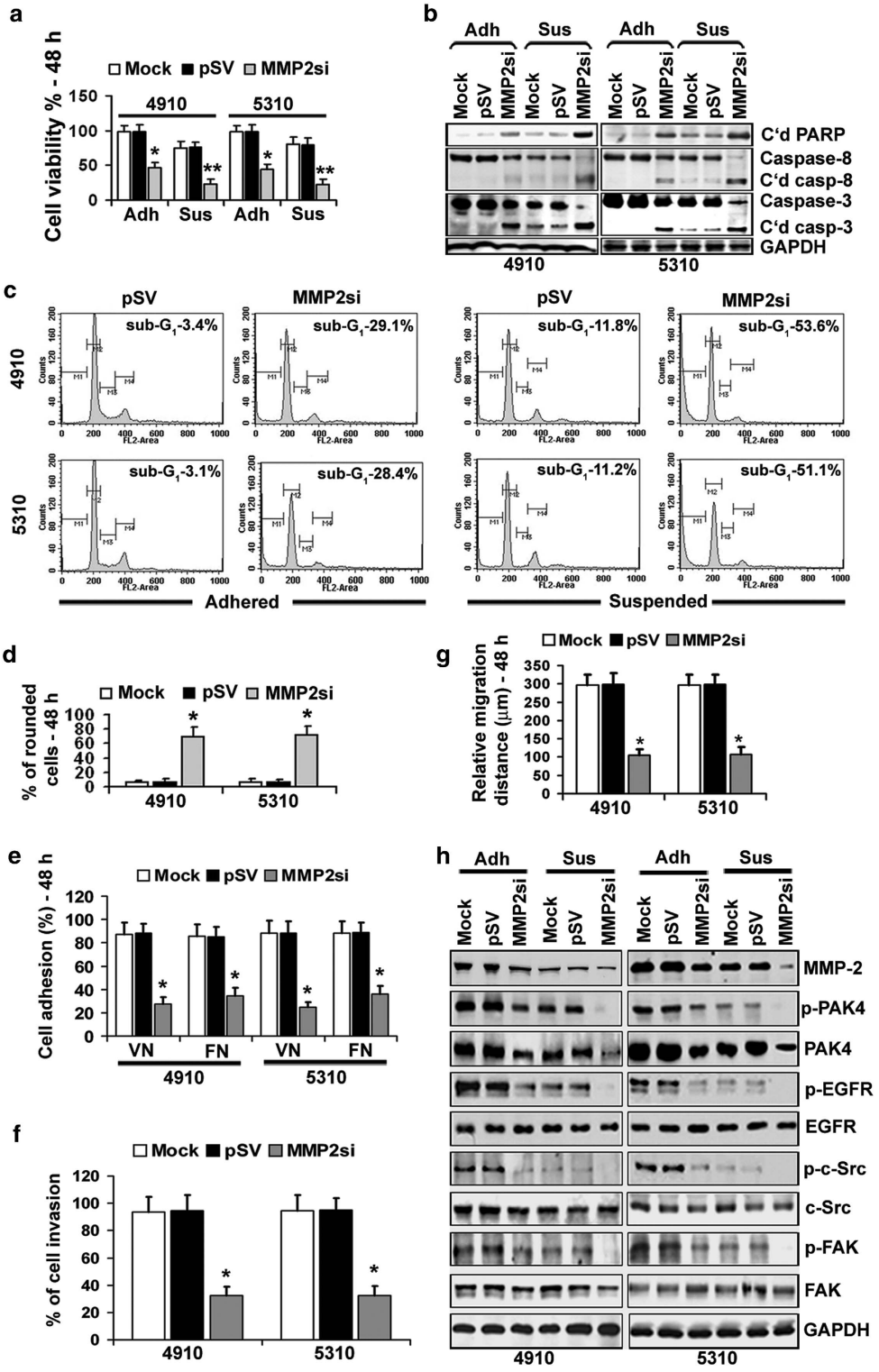

Figure 1 MMP-2 deficiency sensitizes human glioma xenograft cells to anoikis and inhibits tumor cell adhesion, invasion and migration. (**a**) The percentage of cell viability was determined with CytoTox-Glo Cytotoxicity Assay kit and the mean ± S.E. values from three repetitions were plotted. Significant differences among different treatment groups were represented by $^{*}P<0.05$ and $^{**}P<0.01$. (**b**) Western blotting was performed using whole-cell lysates from adhered (Adh) and suspended (Sus) cells. GAPDH served as a loading control. (**c**) FACS analysis (10 000 events) with propidium iodide staining confirmed the enhanced anoikis sensitization in MMP2si-treated cells. Different phases of cell cycle in the histogram are represented by M1: sub-/G1, M2: G1, M3: S and M4: G2/M. The percent of apoptotic cells (sub-G1) was highlighted and experiment was repeated thrice to verify the results. (**d**) Percent of rounded cells were plotted as mean ± S.E. obtained from three individual experiments ($^{*}P<0.01$). (**e**) Cell adhesion experiments were performed on vitronectin (VN)- and fibronectin (FN)-coated plates as described in Materials and Methods. Percentage of cell adhesion was plotted as mean ± S.E. obtained from three experimental replicates ($^{*}P<0.01$). (**f**) Percentage of cell invasion through matrigel-coated transwells was depicted as mean ± S.E. obtained from three independent experiments ($^{*}P<0.01$). (**g**) Relative wound-healing migration distances were measured and plotted in the form of mean ± S.E. values obtained from three replicates ($^{*}P<0.01$). (**h**) Whole-cell lysates were subjected to western blotting

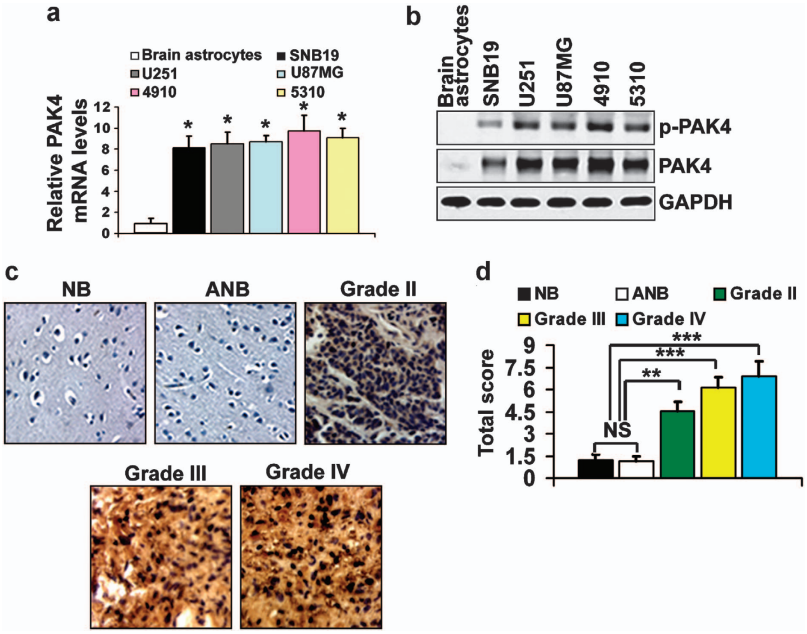

Figure 2 PAK4 is upregulated in glioblastoma. (**a**) Quantitative RT-PCR was performed as described in Materials and Methods and relative PAK4 mRNA levels normalized to internal GAPDH controls were plotted as mean ± S.E. values from three repetitive experiments. Significance was denoted by (*$P<0.01$). (**b**) Immunoblotting was performed using whole-cell lysates, and GAPDH served as a loading control. (**c**) Immunohistochemical analysis using Human Glioma Tissue Microarray indicates the PAK4 expression pattern in normal brain (NB), cancer-adjacent normal brain (ANB) and human glioma tissues of different pathological grades. (**d**) Number of PAK4 positive cells was scored in randomly selected microscopic fields and plotted as mean ± S.E. Significant difference was denoted by **$P<0.01$ and ***$P<0.001$, respectively. NS, not significant

Altered gene expression profile in PAK4 downregulated cells. In an attempt to further identify the possible PAK4 regulation of different essential molecular intermediates participating in tumor cell proliferation, adhesion and anoikis resistance, we analyzed the gene expression levels by performing cDNA-PCR arrays in pSV- and PAK4si-treated 4910 cells. Comparative studies indicated the significant downregulation of various genes which encode essential proteins participating in cell anchorage to ECM and survival, including CDH1, ICAM1, ITGA5, ITGAV, ITGB1, ITGB3, LAMA2, MMP2, CCNB1, CCND1, CHUK, EGFR, GRB2, FOS, MYC, MAPK14, MAX, ILK, RPS6KA1, TIRAP, GATA3, HMGA1, IL10RA, JAK1, NFKB1, STAT1 and STAT5B in PAK4-knockdown cells after 48 h (Figure 3h). Conversely, the potential negative regulators of proliferation, apoptotic proteins and tumor suppressors, including KAL1, CDKN1A, TGFB1, TP53, RB1, CASP9, BAD, PTEN, RBL2, SHC1, SOS1, TCS1, PIAS1, PTPRC, SLA2 and SOCS5, were significantly upregulated in the PAK4si-treated cells compared with pSV-treated controls (Supplementary Table 1).

MMP-2 is a PAK4-interacting protein and decreased PAK4/MMP-2 binding abrogates EGFR signaling in glioma. Significant inhibition in cell adhesion on VN-coated plates and anoikis sensitization in PAK4si-treated cells further prompted us to check the expression levels of $\alpha v\beta 3$ integrin (VN receptor) and other intermediate proteins involved in cell adhesion and proliferation. We observed a substantial decrease in αv, $\beta 3$, MMP-2, phospho-EGFR, EGF, CyclinD1, PCNA and Bcl-xL levels and enhanced cleaved caspase3 in PAK4si-treated cells (Figure 4a). EGFR phosphorylation array revealed a substantial inhibition of 85.5%, 80.1% and 79.8% in phospho-EGFR (Ser1070), phospho-ErbB2 (Thr686) and phospho-ErbB2 (Ser1113) levels, respectively, in PAK4si-treated 4910 cells (Figure 4b). A significant inhibition in phospho-EGFR (Ser1070) (77.6%), phospho-ErbB2 (Tyr1221/1222) (77.1%), phospho-ErbB2 (Thr686) (75.2%), phospho-ErbB2 (Ser1113) (78.2%) and phospho-ErbB4 (Tyr1284) (77.5%) were observed in PAK4si-treated 5310 cells (Figure 4c).

Our independent knockdown experiments using MMP2si and PAK4si suggested a possible functional cooperativity between these proteins. On the basis of cell-adhesion assays, indicating significant inhibition of VN adhesion and decrease in $\alpha v\beta 3$ integrin expression in PAK4si-treated cells, it is interesting to check the possible interaction of PAK4 with MMP-2 (which is a $\alpha v\beta 3$-ligand). Co-immunoprecipitation (co-IP) assays indicated complex formation of PAK4 and MMP-2 in 4910 cells (Figure 4d). Immunoprecipitation with anti-Myc antibody in MMP-2-FL-overexpressing 4910 and 5310 cells also revealed the physical association between PAK4 and MMP-2 proteins (Figure 4e). Further, to identify the specific MMP-2-interacting domain within PAK4, we performed glutathione S-transferase (GST) pull-down assays using biotin-labeled PAK4 truncated mutants and GST-MMP-2. GST-MMP-2 specifically interacted with PAK4 kinase domain (PAK4-KD, 330-591aa). Conversely, MMP-2 binding to other PAK4 domains CRIB and GID was not detected (Figure 4f). The immunoprecipitation experiments with anti-PAK4 and anti-MMP-2 antibodies showed that the PAK4/MMP-2 binding is significantly inhibited in PAK4si-treated 4910 and 5310 cells compared with mock and pSV controls, which showed

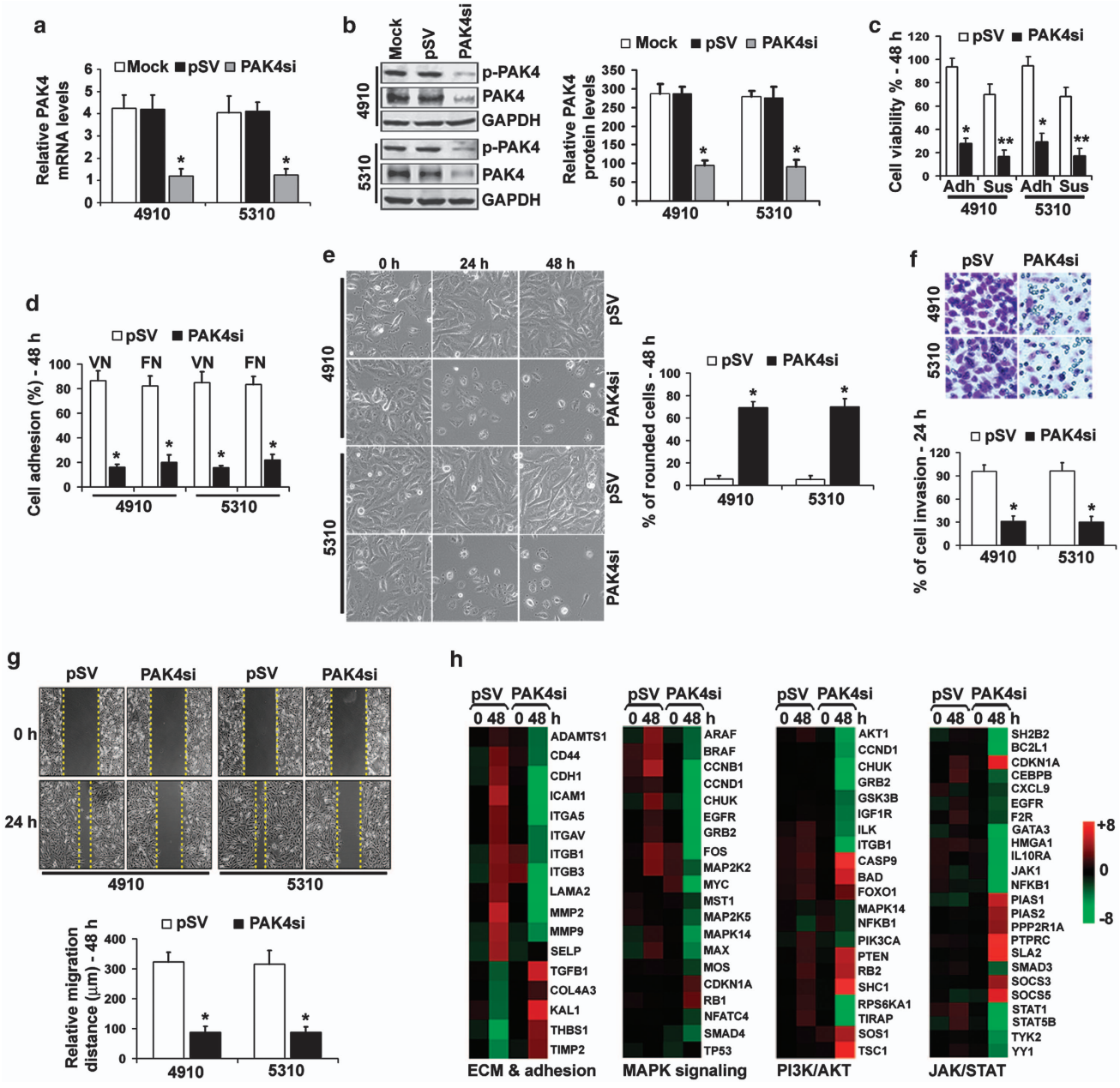

Figure 3 Downregulation of PAK4 inhibits anchorage-independent growth, migration and modulated gene expression profile in glioma xenograft cells. (**a**) Quantitative RT-PCR showing the relative PAK4 mRNA levels normalized to internal GAPDH controls. Mean ± S.E. values obtained from three replicates were presented (*$P<0.01$). (**b**) Whole-cell lysates were subjected to immunoblotting in mock-, pSV- and PAK4si-treated cells after 48 h of transfection. Blots were re-probed with GAPDH to monitor equal loading. Relative PAK4 protein levels were estimated using ImageJ 1.42 (NIH) and plotted as mean ± S.E. values obtained from three independent experiments (*$P<0.01$). (**c**) The 4910 and 5310 cells cultured in adhered (Adh) and suspended (Sus) conditions in 96-well plates were subjected and to pSV and PAK4si treatments for 48 h. The percentage of cell viability was estimated as described in Materials and Methods and plotted as mean ± S.E. values obtained from three repetitive experiments (*$P<0.05$ and **$P<0.01$). (**d**) Percentage of cell adhesion on vitronectin and fibronectin (5 μg/ml each) was determined and graphically represented as mean ± S.E. obtained from three experimental replicates. (**e**) Phase contrast microscopic pictures of pSV- and PAK4si-treated 4910 and 5310 cells (left). The mean ± S.E. values of percentage of rounded cells were plotted in the bar diagram and significance was represented by * at $P<0.01$ (right). (**f**) Transwell matrigel invasion assay depicts the invaded cells in pSV- and PAK4si-treated cells after Hema-3 staining (top). Percentage cell invasion was represented as mean ± S.E. obtained from three experimental replicates, *$P<0.01$ (bottom). (**g**) Wound-healing migration assay was performed as described in Materials and Methods and representative images from three independent experiments were presented (top). The average migration distances were measured using a light microscope with an ocular micrometer and plotted in the form of mean ± S.E. values obtained from three replicates. Significant difference was represented by * at $P<0.01$ (bottom). (**h**) Modulation of gene expression profile in PAK4si-treated 4910 cells in comparison with pSV-treated controls. The cDNA PCR arrays were performed using RT^2 Profiler PCR Array kits (SA Biosciences) for ECM and adhesion; MAPK, PI3K/AKT and JAK/STAT signaling pathways as described in Materials and Methods and relative fold change values obtained from three experimental replicates were represented in the form of heat maps

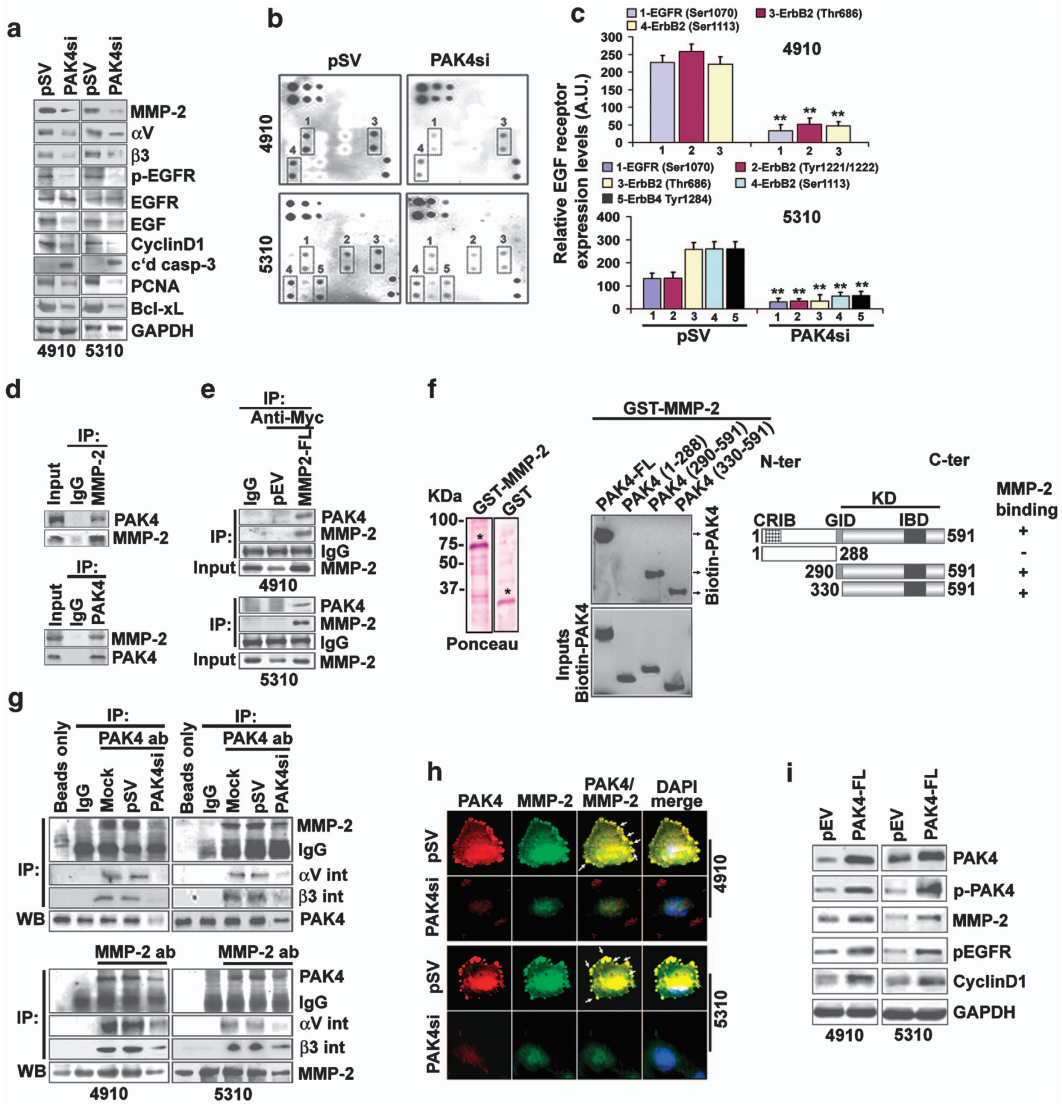

Figure 4 MMP-2 directly interacts with PAK4. (**a**) Western blotting was performed using whole-cell lysates of pSV- and PAK4si-treated cells. (**b**) Modulation of EGF receptor phosphorylation levels after PAK4si treatment in 4910 and 5310 cells. Whole-cell lysates of pSV- and PAK4si-treated cells were subjected to EGFR phosphorylation array and representative array images from three independent experiments were presented. (**c**) Densitometric analysis of EGFR array showing the mean ± S.E. values obtained from three repetitions and significance is denoted by ** at $P<0.01$. (**d**) The formation of a PAK4/MMP-2 complex in 4910 cells was analyzed by co-immunoprecipitation (IP) with whole-cell lysates (500 μg) using specific antibodies against MMP-2 and non-specific IgG. Immunoprecipitates were subjected to western blotting and probed with anti-PAK4 antibody (upper panel). Immunoprecipitation with PAK4 and subsequent immunoblotting with MMP-2 also confirmed the PAK4/MMP-2 complex formation (lower panel). Input samples indicate 10% of pre-immunoprecipitated samples (50 μg). (**e**) The formation of a PAK4/MMP-2 complex in MMP-2-FL-overexpressing cells was analyzed by IP with anti-Myc antibody, followed by immunoblotting using anti-PAK4 and anti-MMP-2 antibodies. (**f**) Identification of MMP-2 interaction domain within PAK4. Bacterially expressed GST and GST-MMP-2 fusion protein were purified using MagneGST Pull-Down System following the manufacturer's instructions, separated on SDS-PAGE and verified by Ponceau staining (left, represented by "*"). Biotin-labeled full-length and truncated mutants of PAK4 were synthesized using a TNT Quick Coupled Transcription/Translation Systems and incubated with GST-MMP-2 (middle-top). The mixtures were washed and elutes were separated by SDS-PAGE, transferred to nitrocellulose membrane and interacting partners were then detected as mentioned in Materials and Methods. Input samples (10% input) were analyzed by SDS-PAGE (middle bottom). Right panel: schematic representations of PAK4 (full length, 1–591 aa) and its truncation mutants (1–288 aa, 290–591 aa and 330–591 aa) used in GST pull-downs to localize the MMP-2 interaction domain within PAK4. Various domains of PAK4 protein are represented by KD (kinase domain), CRIB (Cdc42Hs/Rac-interactive binding domain), GID (GEF–H1 interaction domain) and IBD (integrin-binding domain). (**g**) PAK4 is involved in complex formation with MMP-2 and $\alpha v\beta 3$-integrin in glioma xenograft cells. Co-immunoprecipitation experiments were performed with anti-MMP-2 and anti-PAK4 antibodies. Non-specific IgG or no antibody (beads only) precipitates were loaded as negative controls, and blots were probed with specific antibodies against MMP-2, αv, β3 and PAK4. Representative blots from three independent experiments were presented. (**h**) Representative confocal microscopic images from three independent experiments indicate the expression and colocalization of PAK4 and MMP-2 in pSV- and PAK4si-treated 4910 and 5310 cells. (**i**). Western blotting was performed with whole-cell lysates and representative blots from three experimental replicates were shown

prominent binding of PAK4 and MMP-2 (Figure 4g). Further, reprobing the IP blots with anti-αv and anti-β3 antibodies indicated the binding of αv-integrin and β3-integrin with both PAK4 and MMP-2 in mock and pSV control cells, which is significantly decreased in PAK4-knockdown cells. A high expression and membrane colocalization of PAK4/MMP-2

was observed in pSV controls, which is significantly decreased in PAK4si-treated cells (Figure 4h). In addition, PAK4 also showed membrane colocalization with $\alpha v\beta 3$ integrin in pSV-treated cells, which is significantly inhibited in PAK4si-treated cells (Supplementary Figure S2C). PAK4 overexpression significantly elevated MMP-2, phospho-EGFR and CyclinD1 levels (Figure 4i). Immunoprecipitation with PAK4 antibody also confirmed enhanced PAK4/MMP-2 binding in PAK4-FL-treated cells (Supplementary Figure S3A). These data provide the auxiliary insights into the possible PAK4/MMP-2 functional cooperation in the regulation of $\alpha v\beta 3$/EGFR-mediated cell survival and anoikis escape in glioma.

Crucial role of $\alpha v\beta 3$/EGFR signaling in the PAK4-mediated migration and invasion. To further evaluate the significance of EGF/EGFR activation in PAK4-regulated cell survival, we treated the pSV- and PAK4si-transfected cells with EGF and GW2974. EGF-induced phospho-EGFR, CyclinD1 and Bcl-xL levels were decreased ($\sim$59.6%) in PAK4si-treated cells. Conversely, GW2974 treatment in pSV-treated cells resulted in $\sim$62.1% inhibition in phospho-EGFR, CyclinD1 and Bcl-xL levels, which were further reduced ($\sim$86.3%) in PAK4si-treated cells (Figure 5a). In addition, VN-adhesion-induced $\alpha v\beta 3$-mediated elevation in MMP-2, phospho-PAK4, phospho-EGFR, CyclinD1 and Bcl-xL levels was decreased in PAK4-knockdown cells. On the other hand, $\alpha v\beta 3$-blocking antibody further decreased EGFR survival signaling in PAK4si-treated cells (Figure 5b). The EGF- or VN-adhesion-elevated invasion and migration was decreased up to $\sim$32.5% in PAK4si-treated cells. Conversely, the combination treatments of PAK4si + GW2974 and PAK4si + $\alpha v\beta 3$-blocking antibody drastically reduced the invasive (Figure 5c) and migratory abilities (Figure 5d) in both cells lines. These results were also in correlation with MMP-2 gelatinolytic activity in various treatments (Supplementary Figure S3B). These results imply the potential PAK4 regulation of $\alpha v\beta 3$/EGFR-mediated anoikis resistance and migration in glioma xenograft cells.

Codepletion of PAK4 and MMP-2 led to robust anoikis and severely inhibited $\alpha v\beta 3$/EGFR-mediated migration and invasion. To further assess the PAK4/MMP-2 functional collaboration in the regulation of anoikis escape and malignancy in glioma, we employed the loss-and-gain-of-function approach using MMP2si + PAK4si or MMP2si + PAK4-FL combination treatments. The MMP2si-inhibited MMP-2, phospho-PAK4, phospho-EGFR, CyclinD1 and Bcl-xL levels were reversed by PAK4-FL treatment in both cell lines (Figure 6a). On the other hand, the PAK4/MMP-2 codepletion completely inhibited the expression of these proteins, suggesting the functional collaboration between PAK4 and MMP-2. Cell viability assays in PAK4si- and MMP2si-treated adhered and suspended cultures indicated the significant cell death ($>$85%) upon simultaneous PAK4 and MMP-2 downregulation (Figure 6b). Consistent with these results, FACS analysis showed cell death in MMP2si-treated cells (adhered, $\sim$30%; suspended, $\sim$53%) and PAK4si-treated cells (adhered, $\sim$32%; suspended, $\sim$57%) compared with respective controls (Figure 6c). Further, PAK4/MMP-2 cosuppression significantly exacerbated cell death (adhered: $\sim$58%; suspended: $\sim$82%) and confirmed that the simultaneous PAK4 and MMP-2 downregulation leads to robust anoikis in both 4910 and 5310 cells. In addition, PAK4-FL-induced invasive and migratory potential of 4910 and 5310 cells was severely inhibited by cosuppression of PAK4 and MMP-2 (Figure 6d and e). These results imply the essential role of direct physical and functional

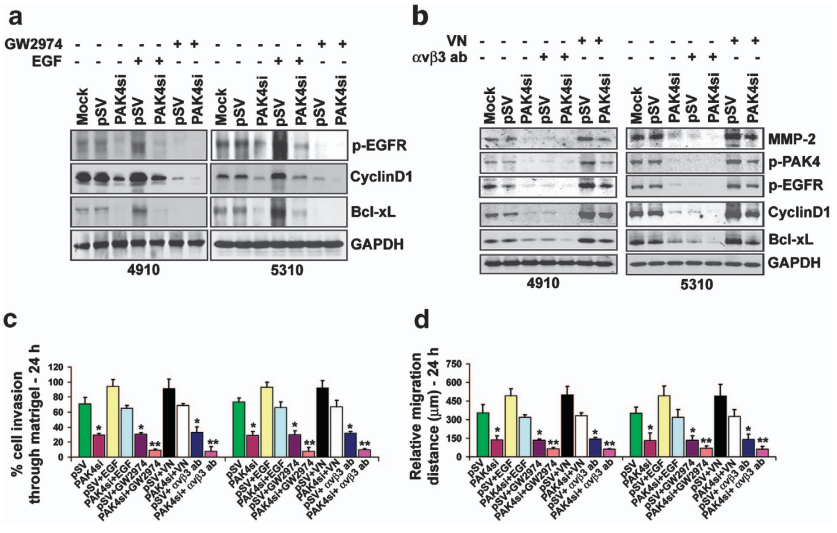

Figure 5 Functional collaboration between PAK4 and MMP-2 in the regulation of $\alpha v\beta 3$/EGFR-mediated migration and invasion in glioma. (**a**) 4910 and 5310 cells were treated with mock, pSV and PAK4si as described in Materials and Methods. At 24 h post-transfection cells were further treated with EGF (2 μg/ml) and GW2974 (10 μM) and incubated for another 24 h. Western blotting was performed using whole-cell lysates and GAPDH served as loading control. (**b**) Combination treatments were performed with VN (5 μg/ml) and $\alpha v\beta 3$ integrin-blocking antibody (5 μg/ml) as described above and representative blots form three independent experiments were shown. (**c**) Percentage of cell invasion obtained from three independent experiments were plotted in the bar diagram ($^*P<0.05$ and $^{**}P<0.01$). (**d**) The relative migration distance values in wound-healing migration assays were plotted as mean ± S.E. values obtained from three individual repetitions ($^*P<0.05$ and $^{**}P<0.01$)

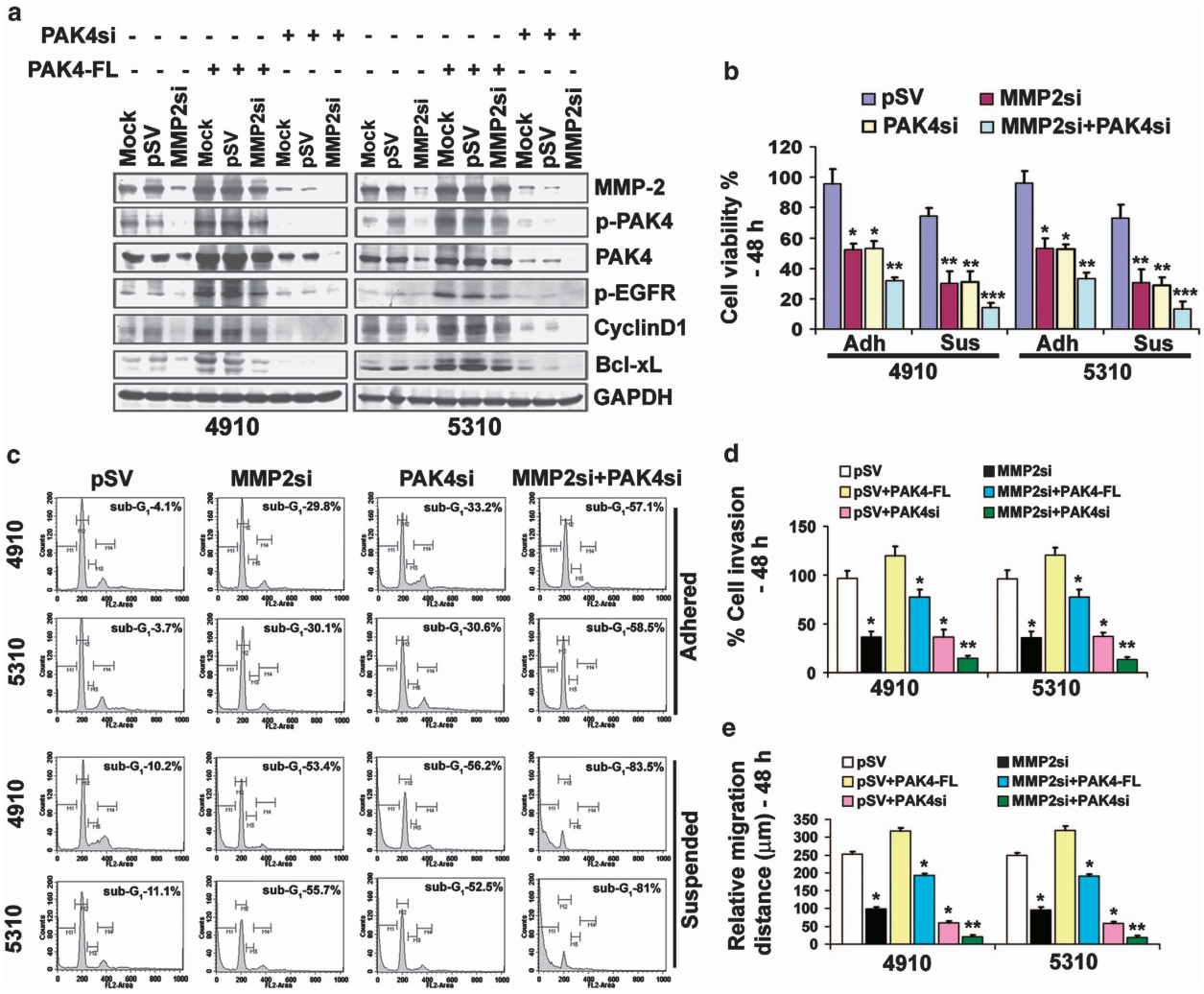

Figure 6 Codepletion of PAK4 and MMP-2 significantly decreased cell invasion and migration and resulted in robust anoikis in glioma xenograft cells. (**a**) Western blotting was performed using whole-cell lysates, and GAPDH was used to monitor equal loading. (**b**) Percentage of cell viability was determined using CytoTox-Glo Cytotoxicity Assay kit and represented as mean ± S.E. values obtained from three experimental replicates (*$P<0.05$, **$P<0.01$ and ***$P<0.001$). (**c**) FACS analysis shows the percent of apoptotic cells (sub-G_1 %) was determined from three individual experiments. (**d**) The percentage of cell invasion was determined from three repetitions and was plotted in the bar diagram as mean ± S.E. (*$P<0.05$ and **$P<0.01$). (**e**) The mean ± S.E. of relative migration distance values obtained from three experimental replicates were plotted in the bar diagram and significant difference was denoted by * and ** at $P<0.05$ and $P<0.01$, respectively

association between PAK4 and MMP-2 in the maintenance of anoikis resistance, migration and invasion in glioma. To determine whether the PAK4 kinase activity is required for rescuing the cells from MMP2si-induced cell death and inhibition in migration and invasion, we used the kinase-dead PAK4-K350M plasmid (Supplementary Figure S4A). PAK4-K350M did not rescue the 4910 cells from MMP2si-induced cell death and loss of invasive and migratory properties (Supplementary Figures S4B and D). Conversely, PAK4-K350M treatment increased cell death and decreased invasion and migration compared with mock controls, suggesting a possible dominant-negative effect of kinase-dead PAK4. These results indicate the requirement of PAK4 kinase activity in the regulation of the EGFR-mediated proliferation, migration and invasion.

Suppression of PAK4 impairs *in vivo* tumor growth in nude mice. Next, the potential oncogenic role of PAK4 was investigated by evaluating the effect of PAK4si on orthotopic tumor growth in nude mice. We observed a significant decrease in the total tumor size in PAK4si-treated tumors (4910, ~52.8%; 5310, ~53.1%) compared with pSV-treated tumors (Figure 7a and b). In addition to the significant suppression of phospho-PAK4 and PAK4 levels, we also observed a decrease in MMP-2 and phospho-EGFR levels in PAK4si-treated tumors (Figure 7c). Further, PAK4si significantly inhibited subcutaneous tumor growth (54.6% in 4910 and 52.5% in 5310 tumors) compared with pSV controls (Supplementary Figures S5A and B). PAK4si decreased phospho-EGFR, β3 integrin and MMP-2 and elevated caspase-3 cleavage, indicating the increased cell death in

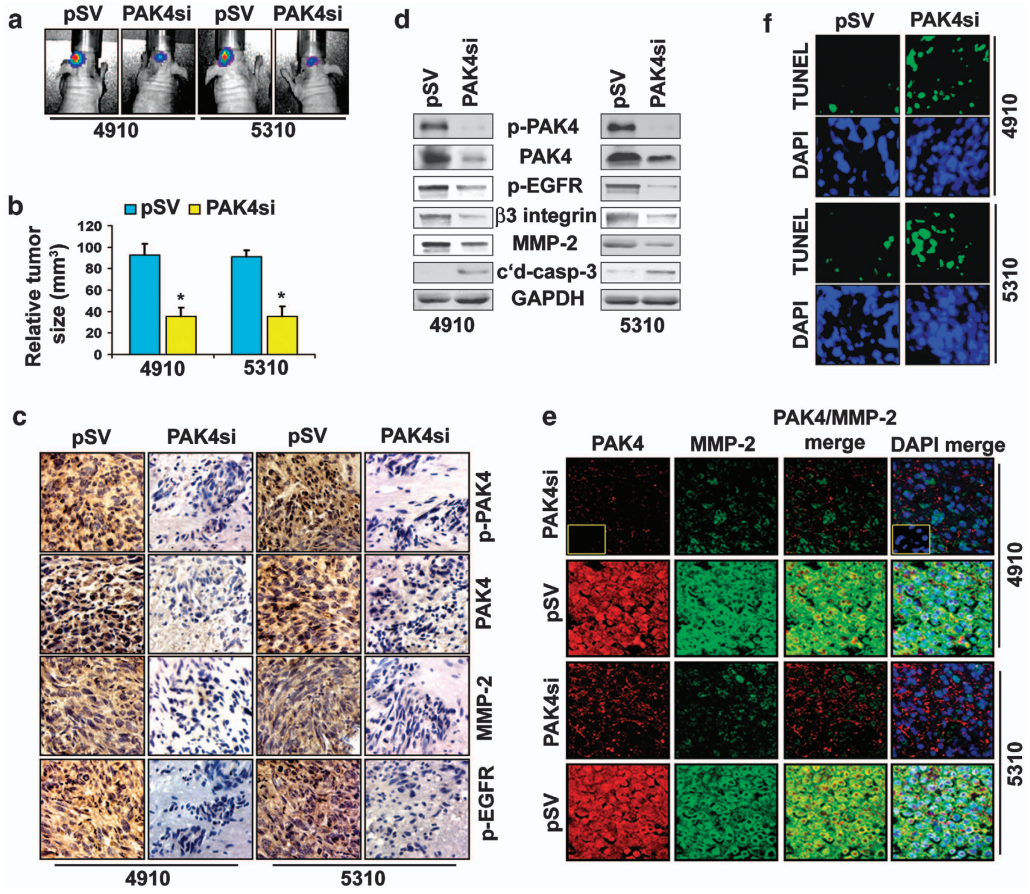

Figure 7 PAK4si suppressed orthotopic tumor growth. (**a**) *In vivo* intracranial tumor experiments were performed with pSV and PAK4si plasmids and representative pictures of tumor growth were presented ($n = 10$). (**b**) The relative brain tumor size in pSV and PAK4si treatments was plotted as mean ± S.E. ($n = 10$, $^*P < 0.01$). (**c**) Immunohistochemical analysis was carried out in pSV- and PAK4si-treated tumors. Nuclei were counterstained with hematoxylin. (**d**) The subcutaneous tumor lysates were subjected to western blotting and representative blots from three independent experiments was presented. (**e**) Immunofluorescence staining depicts the expression and co-localization levels of PAK4 (red) and MMP-2 (green) in pSV- and PAK4si-treated 4910 and 5310 tumor sections. Nuclei were counterstained with DAPI. Insets: 4910 tumor sections stained with non-specific rabbit IgG as negative control. (**f**) TUNEL assay in pSV- and PAK4si-treated tumor sections ($n = 10$). Nuclei were counterstained with DAPI

tumors (Figure 7d). A high expression and strong colocalization of PAK4/MMP-2 (Figure 7e) and PAK4/$\alpha v\beta 3$ were observed in pSV-treated tumors (Supplementary Figure S4C). Conversely, PAK4si inhibited PAK4/MMP-2 and PAK4/$\alpha v\beta 3$ expression and colocalization in both 4910 and 5310 tumors. In addition, terminal deoxynucleotidyl transferase dUTP nick end labeling (TUNEL) assay confirmed the PAK4si-induced cell death in orthotopic tumors (Figure 7f). These *in vivo* results corroborate our *in vitro* findings and highlight the significance of PAK4/MMP-2 functional cooperativity in the regulation of $\alpha v\beta 3$/EGFR survival signaling in glioma.

Discussion

To cope with stress conditions such as hypoxia and inflammation in the extracellular tumor milieu and for maintenance of robust growth and invasiveness, cancer cells exploit constitutive activation of various signaling pathways.[3] Ability to evade anoikis has an important role in cancer cell survival during migration, colonizing foreign tissues and establishment of secondary tumors or advanced-stage cancers.[4] The present study unveils a novel mechanism of PAK4/MMP-2 axis in the regulation of anoikis resistance and metastases in glioma.

PAK proteins are known to regulate cell motility involving focal adhesion dynamics by modulating paxillin.[10] PAK4-knockout embryos displayed abnormalities in heart, vascular and extraembryonic tissue development and showed decreased proliferation and self-renewing ability in neural progenitor cells.[17–20] *In vivo* experiments with PAK4$^{-/-}$ cells showed severe inhibition in tumor growth.[21] Recent studies with PAK4 inhibitors, PF-3758309, LCH-7749944, and several pyrroloaminopyrazole compounds suggested the inhibition of anchorage-independent survival in cell lines and abrogated growth in multiple human xenograft tumors.[22–24] On the other hand, studies with RNAi-mediated PAK4 knockdown also confirmed decreased proliferation, migration and invasion *in vitro* and significantly reduced *in vivo* tumor growth in nude mice, suggesting that the PAK4 knockdown is sufficient to abrogate tumor progression.[25–27] PAK4 overexpression protected cells from different apoptotic stimuli

including radiation, serum deficiency and TNFα-induced cleavage of PARP and caspase-3.[25,26] Studies indicated that PAK4 overexpression promoted cancer cell migration and invasion in c-Src, ERK1/2, EGFR and HGF signaling pathways.[13,26,28] PAK4 has been suggested to function upstream of EGFR, and constitutive PAK4 increased MMP-2 activity and subsequently enhanced migration in ovarian cancer.[13] Our data suggested the direct interaction between PAK4 and MMP-2, and regulation of integrin-mediated EGFR signaling. PAK4 was shown to participate in mitosis by mediating GDP- or GTP-bound Ran phosphorylation and regulate the assembly of Ran-dependent complexes on the mitotic spindle.[29] PAK4 has been implicated in the cell cycle regulation, and an N-terminal PAK4 interaction domain is suggested to facilitate its involvement in ribonucleoprotein complexes.[30,31] PAK4 facilitated β-catenin nuclear translocation by direct binding and increased TCF/LEF activity by coupling with TCF/LEF DNA-binding complex.[32] Role of PAK4 in the regulation of cell adhesion and migration has been reported earlier.[33–36] The NIH3T3 fibroblasts overexpressing active PAK4 (S474E) mutant displayed oncogenic transformation and acquired the potential of anchorage-independent survival, whereas dominant-negative PAK4 inhibited foci formation.[33,36] The 466-572aa region of PAK4 is critical for DiGeorge critical region 6 (DGCR6) binding, and PAK4/DGCR6/β-actin complex was shown to be required for cell migration in gastric cancer.[37]

Our previous studies and that of others indicated the role of MMP-2/αvβ3 interaction in the regulation of tumor proliferation, invasion and angiogenesis.[38,39] Earlier reports demonstrated the role of MMP-2 in cell survival and migratory events by modulating the αvβ3- and α5β1-mediated signaling in glioma.[40,41] Although a large number of MMP broad-spectrum drugs failed in clinical studies, recent studies on the critical roles of MMP-2 in tumors suggests the need for development and assessment of specific MMP-2 targeting drugs.[42–44] PAK4 has been shown to directly interact with the membrane-proximal region of integrin β5 and modulate αvβ5-mediated cell migration in human breast carcinoma.[33,35] Redistribution of cytoplasmic PAK4 to membrane lamellipodea precedes its direct complexing to αvβ5-integrin but not to β1-integrin (FN receptor) upon VN adhesion. Our results indicated that MMP-2 (a αvβ3-ligand) is a new PAK4-interacting protein and PAK4/MMP-2 complex formation augmented αvβ3-integrin-mediated EGFR pathway activation, which confers anoikis resistance in the glioma xenograft cell lines. The GST pull-down experiments confirmed the binding of MMP-2 to PAK4-KD. The kinase domain of PAK4 comprises an ATP-binding domain and a c-terminal integrin-binding domain (IBD), which facilitates binding and subsequent phosphorylation of β5 integrin and is suggested to regulate tumor-cell motility.[33–36] Our present data suggesting the MMP-2 direct binding to PAK4-KD (which comprises IBD) further provides interesting insights into the potential functional coupling of PAK4/MMP-2 complex to integrin proteins and possible regulation of integrin-mediated pathways in cancer.

MMP-2 knockdown rendered glioma cells to apoptosis by cleavage of PARP, caspase-8 and caspase-3.[41,45] Our previous studies on MMP-2 knockdown indicated the suppression of p65 nuclear translocation by decreasing TRADD-TNFR1 binding and led to Fas/c-Jun-mediated apoptosis by elevating TNFR1-FADD binding and death complex formation.[41] PAK4 has also been shown to facilitate the appropriate TRADD binding with the TNFR complex in a kinase-dependent or -independent manner and is suggested to activate NF-κB and ERK pro-survival pathways, thus gaining attention in tumor studies.[25] These studies imply that PAK4 and MMP-2 act as upstream signaling molecules in the regulation of TRADD-TNFR-mediated NF-κB activation and subsequent target gene expression in tumors. Several independent studies suggested the key role of PAK4 and MMP-2 proteins in the regulation of essential pathways of cell proliferation, migration and invasion.[14,19,21,25,26,28,40,41,45,46] Inhibition of either PAK4 or MMP-2 resulted in the down-regulation of both the molecules. However, simultaneous depletion of both PAK4 and MMP-2 led to significant anoikis-mediated cell death and severe inhibition in cell migration by downregulating αvβ3-mediated EGFR pathway activation. Overexpression of kinase-dead PAK4 showed a dominant negative effect on cell death, suggesting that the regulation of EGFR-mediated signaling activation is dependent on PAK4 kinase activity in glioma. Our results are in corroboration with the previous reports demonstrating the dominant negative role of kinase-dead PAK4 plasmid.[12,18,26,47,48]

In summary, we demonstrate that the PAK4 is upregulated in glioma. Our GST pull-down experiments indicated MMP-2 as a PAK4-interacting protein and identified the PAK4-KD as MMP-2-binding domain. In addition, αvβ3 antibody and EGFR-blocking experiments further confirmed the potential role of αvβ3 and EGFR as potential mediators in the regulation of PAK4/MMP-2 survival axis. PAK4 suppression resulted in impaired tumor growth due to cell death in orthotopic tumor experiments. Our results highlight the functional cooperativity between PAK4 and MMP-2 by direct interaction in the regulation of anoikis resistance and metastases, and thereby provide a biological basis for potential future therapeutic significance of dual targeting of PAK4 and MMP-2 in the glioma treatment.

Materials and Methods

Cell culture, reagents and antibodies. Human glioma xenograft cell lines 4910 and 5310 (generously provided by Dr. David James, University of California at San Francisco), which are highly invasive in mouse brain, were generated and maintained in nude mice.[49] These cells were cultured in RPMI 1640 medium (Mediatech Inc., Herndon, VA, USA) supplemented with 10% FBS (Invitrogen Corporation, Carlsbad, CA, USA), 50 units/ml penicillin and 50 μg/ml streptomycin (Life Technologies, Inc., Frederick, MD, USA) in a CO_2 chamber. Human GBM cell lines SNB19, U251 and U87 (American Type Culture Collection, Manassas, VA, USA) were grown in RPMI 1640 containing glutamate (5 mM), 10% FBS and penicillin/streptomycin. Human brain astrocytes were purchased (Sciencell Research Laboratories, Carlsbad, CA, USA) and cultured in astrocyte medium augmented with 2% FBS, 1% penicillin/streptomycin and 1% astrocyte growth supplements. We used specific antibodies against PAK4, phospho-PAK4 (Ser474), MMP-2, αv-integrin, β3-integrin, caspase-3, caspase-8, EGF, EGFR, PARP, PCNA, phospho-EGFR (Tyr1068), c-Src, FAK, phospho-FAK (Ser722), Bcl-xL, CyclinD1, GAPDH and HRP-conjugated secondary antibodies (Santa Cruz Biotechnology, Santa Cruz, CA, USA) and Alexa Fluor-conjugated secondary antibodies (Life Technologies). We also used phospho-c-Src (Tyr416) and anti-Myc antibodies (Cell Signal Technology, Boston, MA, USA). Additionally, EGFR/ErbB2 dual inhibitor-GW2974 (Sigma Aldrich, St. Louis, MO, USA), recombinant human-EGF protein and αvβ3-integrin function-blocking antibody (clone 23C6, Millipore Inc., Billerica, MA, USA) were used in the present study.

Human tumor samples. Human Glioma Tissue Microarray (U.S. Biomax Inc., Rockville, MD, USA) containing glioma tissue samples of various pathological grades (WHO grade I, grade-II (low grade gliomas), grade-III (anaplastic astrocytomas and oligodendrogliomas) and grade-IV (GBM), total 33 cases/63 cores), normal brain (NB) tissues and cancer-adjacent normal brain (ANB) tissues were used in the present study. In addition, NB and clinically classified brain tumor biopsies (grade-II ($n=17$) and grade-IV ($n=15$)) were obtained during autopsies of glioma patients within 24 h of death or from patients who underwent surgery at OSF Saint Francis Medical Center, Peoria, IL, USA. All samples were collected under protocols approved by the University of Illinois College of Medicine (Peoria, IL, USA) Institutional Review Board.

Plasmids and transient transfection experiments. The full-length PAK4 was amplified using PAK4-sense, 5′-ATGTTTGGGAAGAGGAAGA-3′ and PAK4-antisense 5′-TCATCTGGTGCGGTTCTGGCGCATG-3′ primers and cloned in pcDNA3.1 (+)/Myc-His-A at *Eco*RI and *Xba*I sites to construct a PAK4 overexpression plasmid (PAK4-FL). The kinase-dead PAK4-K350M plasmid[12] and siRNA-insensitive MMP-2 overexpression plasmid (MMP-FL) were also used.[45] On the other hand, MMP-2 knockdown was achieved by using pcDNA3.0 plasmid containing MMP-2 siRNA (MMP2si) as described earlier.[41] The PAK4-targeting siRNA sequence (5′-TCGAGACCAGCACGAGCAGAAGTTC*GGAATTCG* GAACTTCTGCTCGTGCTGGTCTTTTT-3′) was designed and cloned in pcDNA3.0 (PAK4si). For transient transfections, cells were seeded in (1×10^4 cells per well) six-well flat-bottom culture plates to grow as a monolayer. In parallel, cells were also cultured in six-well ultra-low attachment plates (Corning Costar, Cambridge, MA, USA) to facilitate anchorage-independent growth in suspension. Independent transient transfection studies were performed in 6-h, serum-starved 4910 and 5310 cells with 2 μg of PAK4si or MMP2si plasmids using the FuGene 6 transfection reagent following the manufacturer's instructions (Roche Applied Science, Indianapolis, IN, USA). The corresponding control treatments with mock ($1\times$ PBS), empty (pEV) and specific scrambled (pSV) vectors were also performed. For different combination treatments, the medium was aspirated from PAK4si- or MMP2si-treated culture plates after 24 h of transfection and cells were further treated with PAK4-FL or MMP2-FL or PAK4-K350M or EGF (2 μg/ml) or GW2974 (10 μM) or $\alpha v\beta 3$-integrin-blocking antibody (5 μg/ml) for another 24 h.

Real-time PCR and cDNA PCR array. Quantitative RT-PCR was performed in cell lines and tumor samples using PAK4: sense, 5′-ATGTTTGG GAAGAGGAAGAAG-3′ and PAK4-antisense, 5′-GGAGTTGGAGCGTGTCAC-3′; GAPDH-sense, 5′-GGAGTCAACGGATTTGGTCGTAT-3′ and GAPDH-antisense, 5′-GTCTTCACCACCATGGAGAAGGCT-3′, respectively.[45] Data were normalized to internal GAPDH levels. Possible modulation of gene expression profile in PAK4-knockdown cells was verified by subjecting the cDNAs of pSV- and PAK4si-treated 4910 cells to different PCR arrays including ECM and adhesion (PAHS013), MAPK signaling (PAHS061), PI3K/AKT signaling (PAHS058) and JAK/STAT signaling (PAHS039) RT^2 Profiler PCR Array kits following the manufacturer's protocol (SA Biosciences, Frederick, MD, USA). The following PCR conditions were used: 1 cycle of 95 °C for 10 min and 40 cycles of 95 °C for 15 s, 60 °C for 30 s, 72 °C for 30 s, followed by 1 cycle of 72 °C for 10 min. Data obtained from three experimental replicates were analyzed using iCycler IQ version 3.1 software (Bio-Rad Laboratories, Hercules, CA, USA) and Ct values were converted into fold change of expression with 2-$\Delta\Delta$Ct method (where $\Delta\Delta CT = \Delta CT$ treatment $-$ ΔCT control). Magnitude of the gene expression changes were determined by fold change values using web-based analysis software and represented by heat maps (http://pcrdataanalysis.sabiosciences.com/pcr/arrayanalysis.php).[45,50]

WB, gelatin-zymography, co-IP and EGFR phosphorylation array. WB and gelatin-zymographic analyses were performed exactly as described earlier.[51] Co-IPs were performed with whole cell lysates (500 μg) immunoprecipitated with anti-PAK4, anti-MMP-2, anti-Myc or non-specific IgG antibodies using μMACS protein-G microbeads and MACS separation columns following the manufacturer's instructions (Miltenyi Biotec, Auburn, CA, USA). Pre-immunoprecipitated input samples (50 μg, 10% inputs) were subjected to WB to check the antibody specificity.

EGFR phosphorylation array. EGF receptor phosphorylation levels were estimated in whole-cell lysates with RayBio Human EGFR Phosphorylation Antibody Array#1 following the manufacturer's instructions (Ray Biotech, Norcross, GA, USA). The average signal intensity of each phospho-EGFR protein dotted in duplicate on the array was estimated by densitometry in three independent experiments.

***In vitro* transcription, translation and GST pull-down experiments.** Different truncated mutants of PAK4 protein were *in vitro* synthesized from specific PCR fragments using Transcend Biotin-Lysyl-tRNA and TNT Quick Coupled Transcription/Translation System (Promega Corporation, Madison, WI, USA) following the manufacturer's instructions. The full-length MMP-2 cDNA (at *Eco*RI and *Sal*I) was sub-cloned in pGEX-5X-1 (GE Healthcare, Piscataway, NJ, USA) and transformed into *E. coli* (DH5α), confirmed by sequencing, following the induction of log-phase cultures in LB media with 1 mM IPTG for 6–12 h at 30 °C.[52] The GST-tagged MMP-2 fusion protein was purified using MagneGST Pull-Down System (Promega) following the manufacturer's protocol. The GST-MMP-2 and GST were immobilized on MagneGST particles and aliquotes of diluted protein-packed GST beads ($\sim$2 μg) were incubated with biotin-labeled PAK4 truncated mutants overnight at 4 °C on an end-to-end rotator. Beads were washed thoroughly and eluted in 20 μl of pre-heated sample buffer, separated by SDS-PAGE, transferred to nitrocellulose membrane and detected using Transcend Non-Radioactive Translation Detection Systems following the manufacturer's protocol (Promega).

Cell viability, colony formation and anoikis assay. Cell viability was determined by CytoTox-Glo cytotoxicity assay following the manufacturer's protocol (Promega). Clonogenic assay was performed as described earlier.[45] After different treatments, cell death was assessed by estimation of percentage of apoptotic cells in sub-G1 phase using propidium iodide staining and FACS analysis (BioSure, Grass Valley, CA, USA).[41] Samples were analyzed on Becton-Dickinson FACS Calibur Flow Cytometer (BD Biosciences, Heidelberg, Germany) using Cell Quest software (BD Biosciences).

Cell adhesion, wound-healing migration and matrigel invasion assays. For the cell adhesion assay, after different treatments, cells (1×10^4) were trypsinized and re-plated on VN- or FN-coated (5 μg/ml) 24-well plates. After 2 h, plates were washed gently and attached cells were Hema-3 stained, microscopically counted and percentage of cell adhesion was determined. For wound-healing migration assay, cells were seeded in six-well plates (1×10^4 cells/well) and treated for 48 h as described above. Considering this point as 0 h, a straight scratch was made in individual wells using a 200-μl pipette tip. After 12 h, the plates were observed for wound healing and the average migration distance of the cells was measured using a microscope calibrated with an ocular micrometer. On the other hand, transwell-matrigel invasion assays were performed and percentage of cell invasion was determined as described earlier.[40]

Immunofluorescence, Immunohistochemistry and TUNEL analyses. For immunofluorescence analyses, at the end of the treatments, the 4910 and 5310 cells in four-well chamber slides (1×10^3 per well) were fixed, permeabilized and incubated with respective primary and Alexa Fluor-conjugated secondary antibodies and subsequently mounted. For nuclear counterstaining, 4′-6-diamidino-2-phenylindole (DAPI) was used. For immunohistochemical analysis, deparaffinized tissue sections (4–5 μm) were blocked in 3% BSA in $1\times$ PBS and incubated overnight at 4 °C with respective primary antibodies followed by incubation with Alexa Fluor/HRP-conjugated secondary antibodies for 1 h at room temperature. Sections were subsequently counterstained with DAPI, mounted and observed under confocal microscope. For DAB (3,3′-diaminobenzidine) staining, hematoxylin was used for nuclear staining, mounted and pictured under light microscope.[45] Total scores of intensity of protein expression and cellular positivity were determined from different microscopic fields.[53] TUNEL assay was performed in the tissue sections as explained earlier.[45]

***In vivo* animal experiments.** Luciferase expressing 4910 and 5310 cells were stereotactically injected (1×10^6 cells/10 μl per mouse) into 4- to 6-week-old female *nu/nu* mice brains as described earlier.[40] Tumors were allowed to grow for 10 days. The animals were divided into four different groups ($n=10$) and Alzet osmotic pumps (model 2004, ALZET Osmotic Pumps, Cupertino, CA, USA) were implanted for the delivery of pSV and PAK4si plasmids (dose: 6–8 mg/kg body weight). An intraperitoneal injection of 2.5 mg of D-luciferin sodium salt (Gold Biotechnology, St. Louis, MO, USA) suspended in 50 μl of PBS was given to the animals, and tumor growth was monitored using IVIS-200 Xenogen imaging system (Xenogen Corporation, Alameda, CA, USA). At the end of the 60 days experiment, all animals were euthanized and brains were

excised, fixed in 10% buffered formalin and paraffin embedded. The tissue sections (5 μm) were subjected to hematoxylin and eosin staining to visualize tumor development, and total tumor volumes were calculated from three independent experiments and plotted as described previously.[45] For subcutaneous tumor experiments, 1×10^6 cells mixed with matrigel were implanted into flanks of mice. After 10 days, the tumors (>5 mm) were treated with pSV and PAK4si plasmids (150 μg) on alternate days for a total of four injections. Tumor volumes were measured with a caliper at 5-day interval. At the end of 30 days experiment, subcutaneous tumors were excised and tumor lysates were immunoblotted.[53] Total tumor volume was calculated using the formula $1/6\Pi$ $(R_{max}) \times (R_{min})^2$, where R_{max} and R_{min} are the maximum and minimum tumor radii respectively.

Statistical analysis. Data from three independent experiments were represented as mean $\pm$ S.E. and statistically analyzed with one-way ANOVA using the Neumann–Keuls method of Sigmastat 3.1. Densitometric analysis was performed using ImageJ 1.42 software (NIH, Bethesda, MD, USA). Significant difference was denoted at $^*P<0.05$, $^{**}P<0.01$ and $^{***}P<0.001$.

Conflict of Interest

The authors declare no conflict of interest.

Acknowledgements. We are grateful to Dr. Audrey Minden for providing PAK4-K350M plasmid. We thank Noorjehan Ali and Susan Renner for technical assistance, and Diana Meister and Sushma Jasti for manuscript review. This research was supported by award NS64535-01A2 (to J.S.R.) from the National Institute of Neurological Disorders and Stroke.

Disclaimer

Contents are solely the responsibility of the authors and do not necessarily represent the official views of NIH.

1. Rao JS. Molecular mechanisms of glioma invasiveness: the role of proteases. *Nat Rev Cancer* 2003; **3**: 489–501.
2. Louis DN. Molecular pathology of malignant gliomas. *Annu Rev Pathol* 2006; **1**: 97–117.
3. Douma S, Van LT, Zevenhoven J, Meuwissen R, Van GE, Peeper DS. Suppression of anoikis and induction of metastasis by the neurotrophic receptor TrkB. *Nature* 2004; **430**: 1034–1039.
4. Guadamillas MC, Cerezo A, Del Pozo MA. Overcoming anoikis - pathways to anchorage-independent growth in cancer. *J Cell Sci* 2011; **124**: 3189–3197.
5. Frisch SM, Ruoslahti E. Integrins and anoikis. *Curr Opin Cell Biol* 1997; **9**: 701–706.
6. Han X, Nabors LB. Integrins-a relevant target in glioblastoma. *Eur J Clin Med Oncol* 2010; **2**: 59–64.
7. Haenssen KK, Caldwell SA, Shahriari KS, Jackson SR, Whelan KA, Klein-Szanto AJ *et al.* ErbB2 requires integrin alpha5 for anoikis resistance via Src regulation of receptor activity in human mammary epithelial cells. *J Cell Sci* 2010; **123**: 1373–1382.
8. Chang C, Werb Z. The many faces of metalloproteases: cell growth, invasion, angiogenesis and metastasis. *Trends Cell Biol* 2001; **11**: S37–S43.
9. Kumar R, Gururaj AE, Barnes CJ. p21-activated kinases in cancer. *Nat Rev Cancer* 2006; **6**: 459–471.
10. Molli PR, Li DQ, Murray BW, Rayala SK, Kumar R. PAK signaling in oncogenesis. *Oncogene* 2009; **28**: 2545–2555.
11. Callow MG, Zozulya S, Gishizky ML, Jallal B, Smeal T. PAK4 mediates morphological changes through the regulation of GEF-H1. *J Cell Sci* 2005; **118**: 1861–1872.
12. Abo A, Qu J, Cammarano MS, Dan C, Fritsch A, Baud V *et al.* PAK4, a novel effector for Cdc42Hs, is implicated in the reorganization of the actin cytoskeleton and in the formation of filopodia. *EMBO J* 1998; **17**: 6527–6540.
13. Siu MK, Chan HY, Kong DS, Wong ES, Wong OG, Ngan HY *et al.* p21-activated kinase 4 regulates ovarian cancer cell proliferation, migration, and invasion and contributes to poor prognosis in patients. *Proc Natl Acad Sci USA* 2010; **107**: 18622–18627.
14. Zhang HJ, Siu MK, Yeung MC, Jiang LL, Mak VC, Ngan HY *et al.* Overexpressed PAK4 promotes proliferation, migration and invasion of choriocarcinoma. *Carcinogenesis* 2011; **32**: 765–771.
15. Ahmed T, Shea K, Masters JR, Jones GE, Wells CM. A PAK4-LIMK1 pathway drives prostate cancer cell migration downstream of HGF. *Cell Signal* 2008; **20**: 1320–1328.
16. Huang PH, Xu AM, White FM. Oncogenic EGFR signaling networks in glioma. *Sci Signal* 2009; **2**: re6.
17. Tian Y, Lei L, Cammarano M, Nekrasova T, Minden A. Essential role for the Pak4 protein kinase in extraembryonic tissue development and vessel formation. *Mech Dev* 2009; **126**: 710–720.
18. Qu J, Li X, Novitch BG, Zheng Y, Kohn M, Xie JM *et al.* PAK4 kinase is essential for embryonic viability and for proper neuronal development. *Mol Cell Biol* 2003; **23**: 7122–7133.
19. Tian Y, Lei L, Minden A. A key role for Pak4 in proliferation and differentiation of neural progenitor cells. *Dev Biol* 2011; **353**: 206–216.
20. Nekrasova T, Minden A. Role for p21-activated kinase PAK4 in development of the mammalian heart. *Transgenic Res* 2012; **21**: 797–811.
21. Liu Y, Xiao H, Tian Y, Nekrasova T, Hao X, Lee HJ *et al.* The pak4 protein kinase plays a key role in cell survival and tumorigenesis in athymic mice. *Mol Cancer Res* 2008; **6**: 1215–1224.
22. Murray BW, Guo C, Piraino J, Westwick JK, Zhang C, Lamerdin J *et al.* Small-molecule p21-activated kinase inhibitor PF-3758309 is a potent inhibitor of oncogenic signaling and tumor growth. *Proc Natl Acad Sci USA* 2010; **107**: 9446–9451.
23. Zhang J, Wang J, Guo Q, Wang Y, Zhou Y, Peng H *et al.* LCH-7749944, a novel and potent p21-activated kinase 4 inhibitor, suppresses proliferation and invasion in human gastric cancer cells. *Cancer Lett* 2012; **317**: 24–32.
24. Guo C, McAlpine I, Zhang J, Knighton DD, Kephart S, Johnson MC *et al.* Discovery of pyrroloaminopyrazoles as novel PAK inhibitors. *J Med Chem* 2012; **55**: 4728–4739.
25. Li X, Minden A. PAK4 functions in tumor necrosis factor (TNF) alpha-induced survival pathways by facilitating TRADD binding to the TNF receptor. *J Biol Chem* 2005; **280**: 41192–41200.
26. Siu MK, Yeung MC, Zhang H, Kong DS, Ho JW, Ngan HY *et al.* p21-Activated kinase-1 promotes aggressive phenotype, cell proliferation, and invasion in gestational trophoblastic disease. *Am J Pathol* 2010; **176**: 3015–3022.
27. Park MH, Lee HS, Lee CS, You ST, Kim DJ, Park BH *et al.* p21-Activated kinase 4 promotes prostate cancer progression through CREB. *Oncogene* e-pub ahead of print 2012; doi:10.1038/onc.2012.255.
28. Paliouras GN, Naujokas MA, Park M. Pak4, a novel Gab1 binding partner, modulates cell migration and invasion by the Met receptor. *Mol Cell Biol* 2009; **29**: 3018–3032.
29. Bompard G, Rabeharivelo G, Frank M, Cau J, Delsert C, Morin N. Subgroup II PAK-mediated phosphorylation regulates Ran activity during mitosis. *J Cell Biol* 2010; **190**: 807–822.
30. Baldassa S, Calogero AM, Colombo G, Zippel R, Gnesutta N. N-terminal interaction domain implicates PAK4 in translational regulation and reveals novel cellular localization signals. *J Cell Physiol* 2010; **224**: 722–733.
31. Nekrasova T, Minden A. PAK4 is required for regulation of the cell-cycle regulatory protein p21, and for control of cell-cycle progression. *J Cell Biochem* 2011; **112**: 1795–1806.
32. Li Y, Shao Y, Tong Y, Shen T, Zhang J, Li Y *et al.* Nucleo-cytoplasmic shuttling of PAK4 modulates beta-catenin intracellular translocation and signaling. *Biochim Biophys Acta* 2012; **1823**: 465–475.
33. Li Z, Lock JG, Olofsson H, Kowalewski JM, Teller S, Liu Y *et al.* Integrin-mediated cell attachment induces a PAK4-dependent feedback loop regulating cell adhesion through modified integrin alpha v beta 5 clustering and turnover. *Mol Biol Cell* 2010; **21**: 3317–3329.
34. Li Z, Zhang H, Lundin L, Thullberg M, Liu Y, Wang Y *et al.* p21-activated kinase 4 phosphorylation of integrin beta5 Ser-759 and Ser-762 regulates cell migration. *J Biol Chem* 2010; **285**: 23699–23710.
35. Zhang H, Li Z, Viklund EK, Stromblad S. P21-activated kinase 4 interacts with integrin alpha v beta 5 and regulates alpha v beta 5-mediated cell migration. *J Cell Biol* 2002; **158**: 1287–1297.
36. Qu J, Cammarano MS, Shi Q, Ha KC, de LP, Minden A. Activated PAK4 regulates cell adhesion and anchorage-independent growth. *Mol Cell Biol* 2001; **21**: 3523–3533.
37. Li X, Ke Q, Li Y, Liu F, Zhu G, Li F. DGCR6L, a novel PAK4 interaction protein, regulates PAK4-mediated migration of human gastric cancer cell via LIMK1. *Int J Biochem Cell Biol* 2010; **42**: 70–79.
38. Brooks PC, Stromblad S, Sanders LC, von Schalscha TL, Aimes RT, Stetler-Stevenson WG *et al.* Localization of matrix metalloproteinase MMP-2 to the surface of invasive cells by interaction with integrin alpha v beta 3. *Cell* 1996; **85**: 683–693.
39. Silletti S, Kessler T, Goldberg J, Boger DL, Cheresh DA. Disruption of matrix metalloproteinase 2 binding to integrin alpha vbeta 3 by an organic molecule inhibits angiogenesis and tumor growth in vivo. *Proc Natl Acad Sci USA* 2001; **98**: 119–124.
40. Badiga AV, Chetty C, Kesanakurti D, Are D, Gujrati M, Klopfenstein JD *et al.* MMP-2 siRNA inhibits radiation-enhanced invasiveness in glioma cells. *PLoS One* 2011; **6**: e20614.
41. Kesanakurti D, Chetty C, Bhoopathi P, Lakka SS, Gorantla B, Tsung AJ *et al.* Suppression of MMP-2 attenuates TNF-alpha induced NF-kappaB activation and leads to JNK mediated cell death in glioma. *PLoS One* 2011; **6**: e19341.
42. Coussens LM, Fingleton B, Matrisian LM. Matrix metalloproteinase inhibitors and cancer: trials and tribulations. *Science* 2002; **295**: 2387–2392.
43. Pavlaki M, Zucker S. Matrix metalloproteinase inhibitors (MMPIs): the beginning of phase I or the termination of phase III clinical trials. *Cancer Metastasis Rev* 2003; **22**: 177–203.
44. Zucker S, Cao J. Selective matrix metalloproteinase (MMP) inhibitors in cancer therapy: ready for prime time? *Cancer Biol Ther* 2009; **8**: 2371–2373.
45. Kesanakurti D, Chetty C, Dinh DH, Gujrati M, Rao JS. Role of MMP-2 in the regulation of IL-6/Stat3 survival signaling via interaction with $\alpha5\beta1$ integrin in glioma. *Oncogene* e-pub ahead of print 2012; doi:10.1038/onc.2012.52.
46. Wells CM, Whale AD, Parsons M, Masters JR, Jones GE. PAK4: a pluripotent kinase that regulates prostate cancer cell adhesion. *J Cell Sci* 2010; **123**: 1663–1673.

47. Callow MG, Clairvoyant F, Zhu S, Schryver B, Whyte DB, Bischoff JR *et al.* Requirement for PAK4 in the anchorage-independent growth of human cancer cell lines. *J Biol Chem* 2002; **277**: 550–558.
48. Lu Y, Pan ZZ, Devaux Y, Ray P. p21-activated protein kinase 4 (PAK4) interacts with the keratinocyte growth factor receptor and participates in keratinocyte growth factor-mediated inhibition of oxidant-induced cell death. *J Biol Chem* 2003; **278**: 10374–10380.
49. Giannini C, Sarkaria JN, Saito A, Uhm JH, Galanis E, Carlson BL *et al.* Patient tumor EGFR and PDGFRA gene amplifications retained in an invasive intracranial xenograft model of glioblastoma multiforme. *Neuro-oncol* 2005; **7**: 164–176.
50. Yin G, Alvero AB, Craveiro V, Holmberg JC, Fu HH, Montagna MK *et al.* Constitutive proteasomal degradation of TWIST-1 in epithelial-ovarian cancer stem cells impacts differentiation and metastatic potential. *Oncogene* e-pub ahead of print 2012; doi:10.1038/onc.2012.33.
51. Kesanakurti D, Sareddy GR, Babu PP, Kirti PB. Mustard NPR1, a mammalian IkappaB homologue inhibits NF-kappaB activation in human GBM cell lines. *Biochem Biophys Res Commun* 2009; **390**: 427–433.
52. Kesanakurti D, Chetty C, Maddirela DR, Gujrati M, Rao JS. Essential role of cooperative NF-κB and Stat3 recruitment to ICAM-1 intronic consensus elements in the regulation of radiation-induced invasion and migration in glioma. *Oncogene* e-pub ahead of print 2012; doi:10.1038/onc.2012.546.
53. Sareddy GR, Nair BC, Gonugunta VK, Zhang QG, Brenner A, Brann DW *et al.* Therapeutic significance of estrogen receptor beta agonists in gliomas. *Mol Cancer Ther* 2012; **11**: 1174–1182.

Supplementary Information accompanies the paper on Cell Death and Disease website (http://www.nature.com/cddis)